Anomaly detection in power inverters of electromechanical actuators based on convolutional neural network and long short-term memory cells

Anomaly Detection in Power Inverters of Electromechanical Actuators based on Convolutional Neural Network and Long Short-Term Memory Cells

Chenyang Lai
Energy Department
Politecnico di Milano.
Milano, Italy
chenyang.lai@polimi.it

Piero Baraldi
Energy Department
Politecnico di Milano.
Milano, Italy
piero.baraldi@polimi.it

Aruna
Energy Department
Politecnico di Milano
Milan, Italy
realarn@outlook.com

Leonardo Baldo
Department of Mechanical and Aerospace Engineering
Politecnico di Torino
Torino, Italy
leonardo.baldo@polito.it

Matteo Davide Lorenzo Dalla Vedova
Department of Mechanical and Aerospace Engineering
Politecnico di Torino
Torino, Italy
matteo.dallavedova@polito.it

Gaetano Quattrocchi
Department of Mechanical and Aerospace Engineering
Politecnico di Torino
Torino, Italy
gaetanoq@gmail.com

Enrico Zio
MINES Paris-PSL, CRC
Sophia Antipolis, France
enrico.zio@minesparis.psl.eu
Energy Department, Politecnico di Milano
Milan, Italy
enrico.zio@polimi.it

***Abstract*—In new generation aircraft, traditional hydromechanical and electrohydraulic actuators of flight control systems are replaced by Electro-Mechanical Actuators (EMAs). Ensuring the functionality of an EMA requires to monitor the health state of its components and promptly detect anomalies. This work develops an anomaly detection method for power inverters, which are among the most critical components of EMAs. It is based on a signal reconstruction model trained to reproduce the values of the signal expected under normal conditions. The cumulative Z-Score of the residuals between reconstructed and measured signals is used as anomaly indicator. The signal reconstruction model combines a Convolutional Neural Network (CNN) and Long Short-Term Memory (LSTM) cells. The CNN enables the extraction of features representative of the system health state from the multidimensional time-series of the measured signals of voltage, motor angular speed and motor position. The LSTM cells allows capturing the complex, non-linear temporal dynamics of the extracted features. The anomaly detection method is validated by considering sensor faults and the degradation of the inverter Metal–Oxide–Semiconductor Field-Effect Transistor (MOSFET).**

Keywords—Electro-Mechanical Actuator, Power Inverter, Anomaly Detection, Convolutional Neural Network, Long-Short Term Memory, MOSFET

I. INTRODUCTION

In new aircrafts, such as the "More Electric Aircraft" or the "All Electric Aircraft" [1], traditional hydraulic actuators of flight control systems are progressively replaced by Electro-Mechanical Actuators (EMAs), which offer multiple advantages in terms of modularity, mechanical simplicity, overall weight and fuel efficiency [2]. An EMA typically consists of a servo motor, a power inverter, a control unit and several sensors measuring quantities of interest for its operation. Given the criticality of EMAs for the safety of the aircraft, it is important to promptly detect the onset of anomalies in its components. This work focuses on the power inverter, which is one of the most critical components of the EMA due to its relatively large probability of failure and potential of catastrophic consequences [3].

With regard to anomaly detection of power inverters, in [4], representative features in the time domain are extracted from current signals and used as input of a support vector machine classifier to identify resistance faults at the junction of multiple insulated gate bipolar transistors (IGBTs). In [5], a state observer-based method with an adaptive threshold is proposed for the identification of open-circuit faults from signals measured at the system level. In [6], a fault diagnostic method for the classification of the causes of anomaly in a three-phase voltage source inverter is developed using a fuzzy logic rule-based system. In [7], a sparse autoencoder-based deep neural network is designed to diagnose open-circuit faults in a phase-controlled, three-phase, full-bridge rectifier. In [8], an anomaly detection method based on the computation of average values of the normalized phase currents is built for the detection of open-switch faults.

Most existing anomaly detection methods primarily focus on open- or short-circuit faults in power inverters, resulting in

approaches that are specifically tailored to these fault modes and may overlook other potential faults. Additionally, open- and short-circuit faults are typically identified easily by standard protection systems. Finally, in the case of EMAs, other failure modes than the mentioned ones may arise. In light of this, this study proposes a novel anomaly detection method for power inverters, specifically designed for EMA monitoring applications. This approach aims to detect incipient fault modes that can go unnoticed by current state-of-the-art detection strategies, offering a higher level framework that extends beyond the conventional open- or short-circuit fault scenarios. Specifically, the proposed anomaly detection method is based on a signal reconstruction model, which combines a Convolutional Neural Network (CNN) and Long Short-Term Memory (LSTM) cells for the estimation of the values of the signals expected under normal conditions, and on the computation of the Z-Score [9] of the residuals, i.e. the difference between the values of the measured and reconstructed signals.

Two case studies regarding sensor faults and degradation of MOSFET are considered to verify the performance of the proposed method.

The paper is organized as follows. The problem and objective of the work are described in Section 2. Section 3 presents the anomaly detection method, including the signal reconstruction model and the use of the cumulative Z-score for anomaly detection. Section 4 shows the application of the proposed method on the two case studies. Finally, the conclusions are discussed in Section 5

II. Problem Statement and Formulation

The power inverter of an EMA, as shown in Fig. 1, is here modelled as a component whose input, $X(t) = \big(x_1(t), \dots, x_3(t)\big)$, are the back-electromotive force (back-EMF), phase voltage and motor angular speed and provides in output the phase current signal, $y(t)$. A dataset $D = \{(X^r, y^r)\}, r = 1, \dots, R$ containing R multidimensional time series of input and output signals collected from power inverters of EMAs under normal conditions of operation is available. Each time series contains the evolution of the signals for a short period of time T. The generic element $x_n^r(t)$ indicates the value of the nth input signal of the rth time-series at the tth time instant.

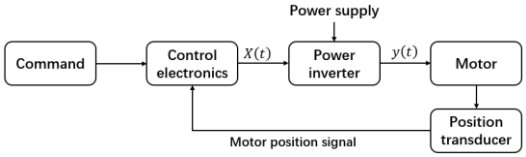

Fig. 1 Structure of EMA.

For the anomaly detection method, a signal reconstruction model is developed and an anomaly indicator is defined. The signal reconstruction model $f(\cdot)$ provides the reconstruction $\hat{y}(t)$ of the output signal $y(t)$ at the tth time instant, i.e. the value of the signal expected for a power inverter operating in normal conditions. The residual between the signal reconstruction and measurement, $res(t) = \hat{y}(t) - y(t)$, is small for EMAs in normal conditions and large in case of anomaly. Therefore, the detection of the occurrence of an anomaly can be based on a statistical analysis of the residuals (Fig. 2).

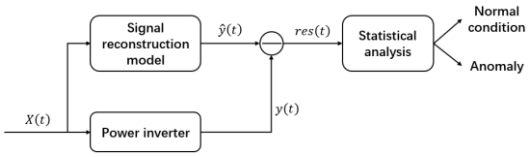

Fig. 2 Anomaly detection based on signal reconstruction.

III. Method

A. CNN-LSTM-based signal reconstruction model

The signal reconstruction model combines CNNs and LSTM cells (Fig. 3). CNNs are employed given their capability of automatically extracting relevant features without human supervision [10]. LSTM cells are well-suited for capturing long- and short-term temporal dependencies in time-series data, thereby effectively modelling complex sequential patterns [11].

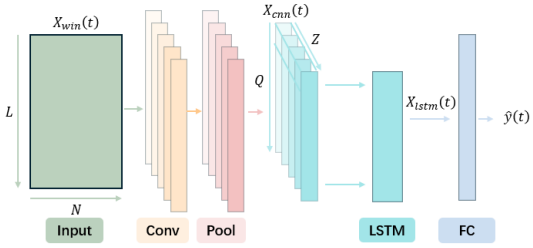

Fig. 3 CNN-LSTM architecture

The model at the current time t receives in input a 3-dimensional time window of length L, $X_{win}(t) = \{X(t - L + 1), \dots, X(t)\} \in \mathbb{R}^{L \times 3}$. To extract features representative of the component health state, CNN layers are applied to map $X_{win}(t)$ into a Z-dimensional time window, $X_{cnn}(t)$, of length Q:

$$X_{cnn}(t) = G_{CNN}(X_{win}(t), \theta_{CNN}) \colon \mathbb{R}^{L \times N} \to \mathbb{R}^{Q \times Z} \qquad (1)$$

with parameters θ_{CNN}. The dimension Z depends on the number and the size of the employed CNN filters and Q depends on the convolutional kernel and stride sizes. Then, LSTM layers are applied to capture the temporal dynamics of the degradation process. Specifically, the mapping:

$$X_{lstm}(t) = G_{LSTM}(X_{cnn}(t), \theta_{LSTM}) \colon \mathbb{R}^{Q \times Z} \to \mathbb{R}^{Q \times H} \qquad (2)$$

with parameters θ_{LSTM} is defined. The working principle of an LSTM layer is shown in Fig. 4 where $x_{cnn}^q(t), q = 1, \dots, Q$ represents the q-th Z-dimensional vector of $X_{cnn}(t)$. The number of LSTM cells is equal to Q, the q-th cell receives $x_{cnn}^q(t)$ as input and produce two H-dimensional vectors: the hidden state vector $h^q(t)$ and the cell state vector $c^q(t)$. Both vectors are, then, passed as input to the $(q + 1)$-th cell in addition to $x_{cnn}^{q+1}(t)$. The output of the LSTM layer is the combination of the hidden state vectors of all LSTM cells $X_{lstm}(t) = [h^1(t), \dots, h^Q(t)], q = 1, \dots, Q$. As a consequence, $X_{lstm}(t)$ contains all temporal information of the time window $[t - L + 1, \dots, t]$.

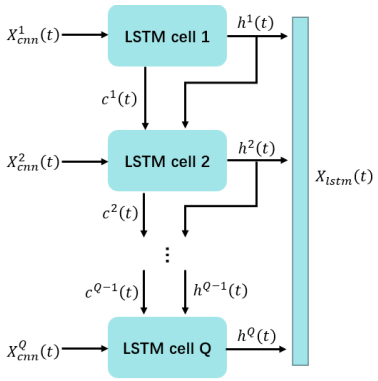

Fig. 4 Working principle of an LSTM layer.

Finally, Fully Connected (FC) layers are used to map the output of the LSTM layer, $X_{lstm}(t)$, into the output signal $\hat{y}(t)$, corresponding to the reconstruction of signal y at time t:

$$\hat{y}(t) = G_{FC}(X_{lstm}(t), \theta_{FC}): \mathbb{R}^{Q\times H} \rightarrow \mathbb{R} \quad (3)$$

The overall signal reconstruction model combines G_{CNN}, G_{LSTM} and G_{FC}:

$$\hat{y}(t) = G_{FC}(G_{LSTM}(G_{CNN}(X_{win}(t), \theta_{CNN}), \theta_{LSTM}), \theta_{FC}): \mathbb{R}^{L\times 3} \rightarrow \mathbb{R} \quad (4)$$

where the parameters $[\theta_{CNN}, \theta_{LSTM}, \theta_{FC}]$ are obtained by minimizing the loss function:

$$Loss = \sum_{t=L}^{T} \|\hat{y}(t) - y(t)\|^2 \quad (5)$$

B. Definition of the anomaly indicator

The anomaly indicator, $A(t)$, is defined as the cumulative Z-Score of the residuals over a time window $[t - L_z + 1, \dots, t]$ of length L_z:

$$A(t) = \sum_{t-L_z+1}^{t} z(t) \quad (6)$$

where $z(t)$ is the Z-Score at time t:

$$z(t) = \frac{res(t) - \mu}{\sigma} \quad (7)$$

with μ and σ indicating the mean and standard deviation of the residuals over a validation set of normal condition data. Notice that the time window used for the computation of the anomaly indicator has a different length, L_z, than that used by the signal reconstruction model given the need of considering different time scales. When $A(t)$ exceeds a threshold thr, an anomaly of the power inverter is detected.

Following the procedure suggested in [12], where μ_2 and σ_2 are the mean and standard deviation of $A(t)$ computed over a second validation set of normal condition data, thr is set as:

$$thr = \mu_2 + 4 \times \sigma_2 \quad (8)$$

IV. Case Studies

The function of the considered three-phase Voltage Source Inverter (VSI) is to generate Alternating Current (AC) and voltage from a Direct Current (DC) voltage source. The VSI consists of six power switches (IGBTs or MOSFETs) arranged in an H-bridge configuration, where each leg of the bridge corresponds to one phase of the AC output (Fig. 5).

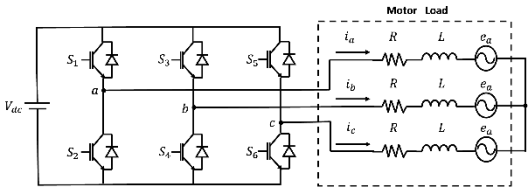

Fig. 5 Scheme of three-phase Voltage Source Inverter (VSI).

In Fig. 5, i_a, i_b and i_c are the electrical currents of each phase, R is the resistance, L is the inductance, and e_a, e_b and e_c are the back-Electromotive Force (back-EMF) of each phase.

A. Hyperparameter setting and performance evaluation criteria

In both case studies, the same architecture of the CNN-LSTM model is used (Table. 1).

TABLE. 1 CNN-LSTM ARCHITECTURE

Layer	Hyperparameters
Input	3 input signals, time window of length $L = 30$
1D Conv	64 filters, kernel size = 5 with Relu activation
1D MaxPooling	Pool size = 2
1D Conv	32 filters, kernel size = 3 with Relu activation
1D MaxPooling	Pool size = 2
LSTM	hidden states size = 128
Dense	64 neurons with Relu activation
Dense	16 neurons with Relu activation
Output	1 neuron (reconstructed signal)

The hyperparameters used for training the CNN-LSTM model are reported in Table. 2. A decay strategy is used to gradually reduce the learning rate, enhancing convergence stability and preventing excessive updating. Additionally, a validation dataset is utilized for early stopping to prevent overfitting by terminating training when the performance on the validation set stops improving.

TABLE. 2 HYPERPARAMETERS USED FOR TRAINING THE CNN-LSTM MODEL

Hyperparameters	Value
Initial learning rate	1e-4
Decay steps	1e5
Decay rate	0.98
Batch size	64
Optimizer	Adam

The performance metrics used to evaluate the accuracy of the signal reconstruction model are the Root Mean Squared Error (RMSE):

$$RMSE = \sqrt{\frac{1}{N_{test}} \sum_{i=1}^{N_{test}} \left(y(i) - \hat{y}(i)\right)^2} \quad (9)$$

and the Mean Absolute Scaled Error (MASE):

$$MASE = \frac{\sum_{i=1}^{N_{test}} |y(i) - \hat{y}(i)|}{\sum_{i=2}^{N_{test}} |y(i) - y(i-1)|} \quad (10)$$

B. *Case study 1*

The dataset is generated by using a high-fidelity EMA model developed by Politecnico di Torino [2]. It consists of 90 trajectories in normal conditions under different operating conditions and 10 trajectories during which a failure of the current sensor is simulated. Table. 3 reports the partition of the dataset into training, validation and test sets.

TABLE. 3 NUMBER OF TRAJECTORIES IN THE TRAINING, VALIDATION AND TEST SETS.

Metrics	Normal	Sensor failure
Training	60	0
Validation	15	0
Test	15	10

LSTM, CNN and Deep Neural Network (DNN) models are considered as comparison methods. The performance on the test set, reported in Table. 4, shows that CNN-LSTM and LSTM significantly outperform both CNN and DNN across all metrics. CNN-LSTM achieves better performance than LSTM on MASE and worse on RMSE. Fig. 6 and Fig. 7 illustrate the reason of this discrepance in the performance. When the motor position gradually and steadily changes (Fig. 6), the CNN-LSTM model significantly outperforms the standalone LSTM due to its ability to capture subtle variations in time. In contrast, Fig. 7 shows a case with abrupt changes in motor position leading to corresponding sharp variations in the current signal. Here, the standalone LSTM performs slightly better, as the CNN-LSTM provides slightly larger relative errors in these extreme cases, which, in turn, notably increase RMSE. Note that the magnitude of this inaccuracy may not be significant when considered in a practical context in relation to the overall scale of the data.

TABLE. 4 PERFORMANCE IN THE RECONSTRUCTION OF NORMAL CONDITION DATA

Metrics	CNN-LSTM	LSTM	DNN	CNN
RMSE [A]	0.109	**0.097**	0.159	0.131
MASE	**1.240**	1.538	2.763	2.047

The proposed method of detecting sensor faults, it has been tested considering 4000 time windows from trajectories in normal conditions followed by 4000 time windows from trajectories with sensor faults. The anomaly indicator (Eq. (6)) has been computed using the hyperparameters of values of Table. 5. As a result, almost all sensor faults can be detected using the cumulative Z-Score as anomaly indicator, without any false alarm (Fig. 8).

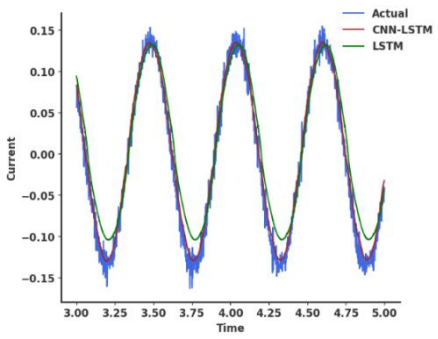

Fig. 6 Signal reconstructions in a transient in which the motor position gradually and steadily changes.

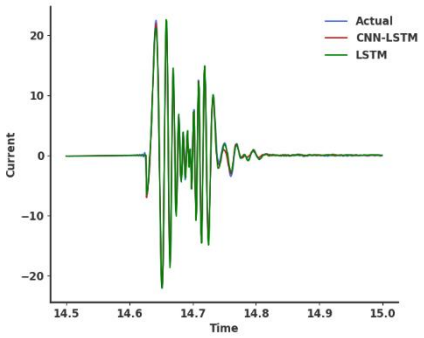

Fig. 7 Signal reconstructions in a transient in which the motor position changes abruptly.

TABLE. 5 PARAMETERS FOR ANOMALY DETECTION BY Z-SCORE.

Parameters	Value
μ	0
σ	0.0037
μ_2	87.78
σ_2	35.07
Threshold	228.05
Length of time window	100

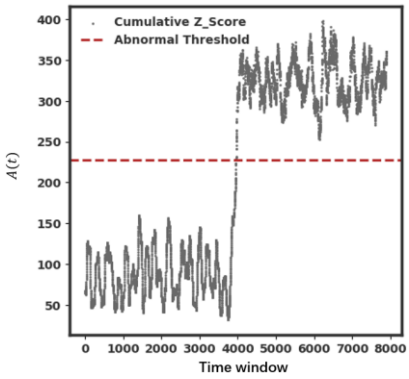

Fig. 8 Evolution of the anomaly indicator. The first 4000 time windows refer to inverters in normal conditions. The last 4000 time windows refer to inverters with a sensor fault. The dashed horizontal line indicates the threshold (thr) for anomaly detection.

C. *Case study 2*

We consider as anomaly the increase of the ON resistance (RDS) of MOSFETs in power inverter. The failure threshold is typically defined as a 50% relative increment of the RDS with

respect to its initial value [3]. A dataset is generated, comprising normal conditions and anomaly with 25%, 35% and 45% increments in RDS using a high-fidelity model of EMA. The sampling frequency for each trajectory is set at 20 kHz, with a simulation duration of 1 second for both normal conditions and anomalies. The dataset consists of 60 trajectories under normal conditions and 30 trajectories for each degradation level. Table. 6 presents the distribution of the dataset into training, validation and test categories.

TABLE. 6 NUMBER OF TRAJECTORIES IN TRAINING, VALIDATION AND TEST SETS.

Metrics	Normal	25%	35%	45%
Training	20	0	0	0
Validation	5	0	0	0
Test	35	30	30	30

The CNN-LSTM model demonstrates high accuracy in reconstructing the current signal expected in normal conditions, achieving an RMSE of less than 0.01 A on normal condition trajectories of the test set, as shown in Fig. 9. Three examples of reconstructed signals in case of anomalies characterized by 25%, 35% and 45% RDS increments and the corresponding residuals are shown in Fig. 10, Fig. 11 and Fig. 12.

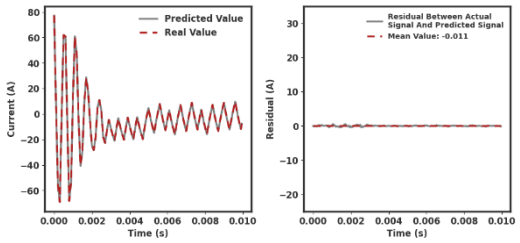

(a) reconstructed signal (b) residuals

Fig. 9 Signal reconstruction of a trajectory in normal conditions.

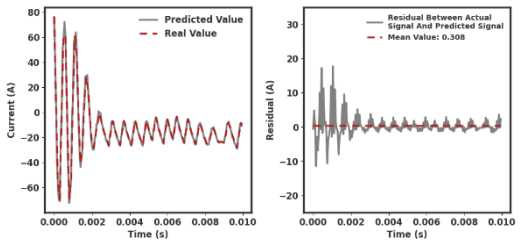

(a) reconstructed signal (b) residuals

Fig. 10 Signal reconstruction of a trajectory with an anomaly characterized by an increment of 25% of RDS.

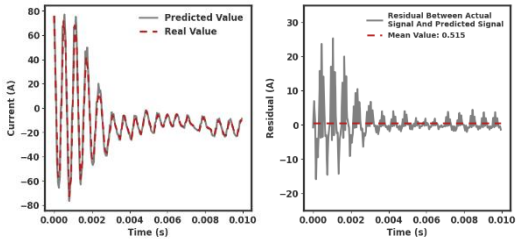

Fig. 11 Signal reconstruction of a trajectory with an anomaly characterized by an increment of 35% of RDS.

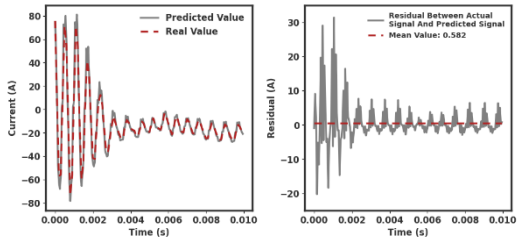

Fig. 12 Signal reconstruction of a trajectory with an anomaly characterized by an increment of 45% of RDS.

It can be seen that the residuals for the case with 25% RDS increment already deviates from 0 allowing to detect the anomaly occurrence. As the RDS increases, the residuals increase accordingly, further reflecting the progressive nature of the degradation.

The values of the hyperparameters used for computing the anomaly indicator are reported in Table. 7. As in the first case study, we consider a test set made of 8000 time-windows, where the first half are taken from trajectories in normal conditions and the remaining from trajectories with an increased RDS. As shown in Fig. 13, all anomalies are detected without false alarms.

TABLE. 7 PARAMETERS FOR ANOMALY DETECTION BY Z-SCORE.

Parameters	Value
μ	0
σ	0.098
μ_2	71.42
σ_2	22.44
Threshold	161.17
Length of time window	100

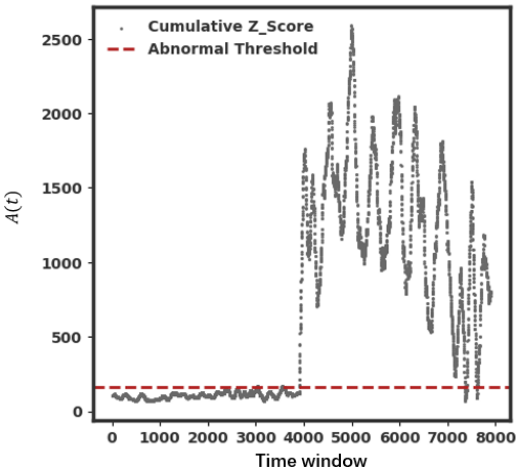

Fig. 13 Evolution of the Z-Score index.

V. CONCLUSIONS

This work has presented an anomaly detection method for power inverters in EMA, which is based on a CNN-LSTM signal reconstruction model and the cumulative Z-score as anomaly indicator. The proposed method is verified through two case studies with failures due to the sensor faults and MOSFET degradation, respectively. The obtained results confirm that the proposed method is able to effectively detect anomalies. Future

work will be devoted to the verification of the method using data collected from real testbench.

ACKNOWLEDGMENT

The authors are thankful to Matteo Bertone for the support on EMA modelling and simulation. The work of Piero Baraldi is supported by FAIR (Future Artificial Intelligence Research) project, funded by the NextGenerationEU program within the PNRR-PE-AI scheme (M4C2, Investment 1.3, Line on Artificial Intelligence). The participation of Chenyang Lai is also supported by CINECA for the computing resources of Class C: RUL-PIDL - HP10CHF7KG. The work of Enrico Zio is supported by the SAFEPOWER project under the HORIZON-CL5-2024-D3-01 call of the European Union, Grant Agreement 101172940. Views and opinions expressed are however those of the author(s) only and do not necessarily reflect those of the European Union or CINEA.

REFERENCES

[1] Dalla Vedova, M. D., Germanà, A., Berri, P. C., & Maggiore, P. (2019). Model-based fault detection and identification for prognostics of electromechanical actuators using genetic algorithms. *Aerospace*, *6*(9), 94.

[2] Berri, P. C., Dalla Vedova, M. D., Maggiore, P., & Viglione, F. (2019). A simplified monitoring model for PMSM servoactuator prognostics. In *MATEC Web of Conferences* (Vol. 304, p. 04013). EDP Sciences.

[3] Yin, Z., Hu, N., Chen, J., Yang, Y., & Shen, G. (2022). A review of fault diagnosis, prognosis and health management for aircraft electromechanical actuators. *IET Electric Power Applications*, *16*(11), 1249-1272.

[4] Bandyopadhyay, I., Purkait, P., & Koley, C. (2018). Performance of a classifier based on time-domain features for incipient fault detection in inverter drives. *IEEE Transactions on Industrial Informatics*, *15*(1), 3-14.

[5] Jlassi, I., Estima, J. O., El Khil, S. K., Bellaaj, N. M., & Cardoso, A. J. M. (2016). A robust observer-based method for IGBTs and current sensors fault diagnosis in voltage-source inverters of PMSM drives. *IEEE Transactions on Industry Applications*, *53*(3), 2894-2905.

[6] Khater, F., El-Sebah, M. I. A., & Osama, M. (2017). Fault diagnostics in an inverter feeding an induction motor using fuzzy logic. *Journal of Electrical Systems and Information Technology*, *4*(1), 10-17.

[7] Xu, L., Cao, M., Song, B., Zhang, J., Liu, Y., & Alsaadi, F. E. (2018). Open-circuit fault diagnosis of power rectifier using sparse autoencoder based deep neural network. *Neurocomputing*, *311*, 1-10.

[8] Zaimen, H., Rezig, A., & Touati, S. (2022). A new detection method of IGBTs open-circuit faults in an induction motor drive. *Turk. J. Comput. Math. Educ*, *13*(2), 748-760.

[9] Altman, E. I., Iwanicz-Drozdowska, M., Laitinen, E. K., & Suvas, A. (2017). Financial distress prediction in an international context: A review and empirical analysis of Altman's Z-score model. *Journal of international financial management & accounting*, *28*(2), 131-171.

[10] Gu, J., Wang, Z., Kuen, J., Ma, L., Shahroudy, A., Shuai, B., ... & Chen, T. (2018). Recent advances in convolutional neural networks. *Pattern recognition*, *77*, 354-377.

[11] Lai, C., Baraldi, P., Quattrocchi, G., Dalla Vedova, M. D. L., Baldo, L., Bertone, M., & Zio, E. (2024, June). Detection of Abnormal Conditions in Electro-Mechanical Actuators by Physics-Informed Long Short-term Memory Networks. In *PHM Society European Conference* (Vol. 8, No. 1, pp. 8-8).

[12] Wang, B., Baraldi, P., Lu, X., & Zio, E. (2020). Fault detection based on optimal transport theory. In *30th European Safety and Reliability Conference, ESREL 2020 and 15th Probabilistic Safety Assessment and Management Conference, PSAM 2020* (pp. 1764-1771). Research Publishing Services.